Hindawi
Mathematical Problems in Engineering
Volume 2021, Article ID 4294985, 12 pages
https://doi.org/10.1155/2021/4294985

Research Article

Numerical Analysis of Cu + Al_2O_3/H_2O Hybrid Nanofluid of Streamwise and Cross Flow with Thermal Radiation Effect: Duality and Stability

Sumera Dero,[1] **Liaquat Ali Lund**,[2] **Zahir Shah**,[3] **Ebenezer Bonyah**,[4] and **Wejdan Deebani**[5]

[1]*Institute of Mathematics and Computer Science, University of Sindh, Jamshoro, Pakistan*
[2]*KCAET Khairpur Mirs, Sindh Agriculture University, Tandojam, Sindh 70060, Pakistan*
[3]*Department of Mathematical Sciences, University of Lakki Marwat, Lakki Marwat 28420, Khyber Pakhtunkhwa, Pakistan*
[4]*Department of Mathematics Education, University of Education Winnebakumasi-(Kumasicompus), Kumasi 00233, Ghana*
[5]*Department of Mathematics, College of Science & Arts, King Abdulaziz University, P.O. Box 344, Rabigh 21911, Saudi Arabia*

Correspondence should be addressed to Ebenezer Bonyah; ebbonya@gmail.com

Received 12 September 2021; Accepted 12 November 2021; Published 2 December 2021

Academic Editor: Ahmed Zeeshan

The motion of water conveying copper and aluminum nanoparticles on a heated moving sheet when thermal radiation and stretching/shrinking surface is significant and is investigated in this study to announce the increasing effects of volume fractions, thermal radiation, and moving parameters on this transport phenomenon. Furthermore, the flow of a Cu − Al_2O_3/water hybrid nanofluid across a heated moving sheet has been studied in both cross and streamwise directions. Thermal radiation effect is also considered, as this effect along with cross flow has not yet been investigated for the hybrid nanofluid in the published literature. Two distinct types of nanoparticles, namely, Al_2O_3 (alumina) and Cu (copper), have been used to prepare hybrid nanofluid where water is considered as a base fluid. The system of nonlinear partial differential equations (PDEs) has been transferred to ordinary differential equations (ODEs) by compatible transformations before solving them by employing the III-stage Lobatto-IIIa method in bvp4c solver in MATLAB 2017 software. Temporal stability analysis has been carried out in order to verify stable branch between two branches by obtaining the smallest eigenvalue values. The branches obtained are addressed in depth against every applied parameter using figures and tables. The results show that there are three ranges of branches, no solution exists when $\lambda > \lambda_c$, dual branches exist when $0.23 \le \lambda \le \lambda_c$, and a single solution exists when $\lambda > 0.23$. Moreover, thermal layer thickness declines initially and then enhances in the upper and lower solutions for the higher values of the thermal radiation parameter.

1. Introduction

Although numerous physical geometries cope with complicated phenomena depending on the industrial requirement, the near-surface flow is still an important aspect of aerodynamics and engineering. In aerodynamics, when the fluid moves on the sheet, the boundary layer which appears from the deformation of streamlines varies from the free flow based on the slope of pressure which is normal to the free flow direction. Pressure found inside the layer of boundary is not influenced by distance from sheet, although certain other characteristics play a part, such as a boundary surface, lower velocity, and smoother curve relative to free-flow velocity. Cross flow is also known as a secondary flow which happens when a component of velocity of the layer is perpendicular to the path of free stream. In such flows, transverse movement is expected to be completely formed. These kinds of flows are used in other technological contexts, such as aircraft, hydraulic, and wind movement phenomena. It seems that Sowerby [1] is the first scholar who studied that boundary layer on the cross flow. After that, the reverse flow of the boundary layer over the moving surface was examined by Klemp and Acrivos [2, 3]. They have concluded that flow consists of three overlapping domains such as the "external uniform flow, a conventional boundary layer with the reverse flow, and an inviscid collision region." Hussaini et al.

[4] considered the upstream moving wall of fluid and solved the modeled equations by Crocco formulation. Moreover, the nonuniqueness of the solutions was noticed. Recently, Altaç et al. [5] studied the mixed convection flow subjected to upward cross flow. Many other significant cross-flow studies can be obtained in these reported research papers [6–10].

In the present decade, the market for lightweight electronic devices and components has risen rapidly, needing more efficient thermal conductivity relative to the simple fluid. Thermal conductivity has a major role in heat transferring between the surface and medium. Technologists and acientists also developed a different form of fluid identified as nanofluid. The word nanofluid has been suggested as micromillimeter-sized particles that are dispersed in the conventional fluid such as water and engine oil [11]. As a consequence, nanofluid thermal conductivity is anticipated to improve heat transfer relative to normal heat transfer fluids [12]. Choi and Eastman [13] suggested the word nanofluid which describes the suspension of solid nanoparticles in the regular fluid. Furthermore, in a study of the flow of 29 nm $CuO - H_2O$ nanofluid over a horizontal surface over the paraboloid of revolution subject to Lorentz force and thermoelectric, it was discovered that maximum temperature distribution with volume fraction is guaranteed at larger values of Lorentz force [14]. Mohamed et al. [15] investigated the effect of viscous dissipation on the $Ag - Al_2O_3$ water-based hybrid nanofluid, discovering that, as the volume fraction increases, so does skin friction. In addition, several experiments have been performed to demonstrate the versatility of nanofluid, taking into consideration different impacts, physical properties, surfaces, and shapes. Collections of nanofluid papers can be found in [16–19].

Researchers became interested in nanotechnology and nanoparticles' research in the last decade of the twentieth century due to their wide range of applications in almost all fields of science. Many researchers conducted several experimental and computational studies in this regard in order to obtain better results in the form of the heat transfer rate. To improve the heat transfer performance of conventional base fluids, solid nanoparticles and base fluids were combined in the preparation of nanofluids as discussed above. Typically, researchers focused on aluminum oxide and copper particles for computational studies due to their good thermophysical properties. Aluminum oxide is used to improve the rheological and filtration properties of drilling fluids because of its high thermal conductivity, which allows it to effectively dissipate heat from the fluid via Brownian motion [20]. Moreover, it is used as a nanoparticle in polymer products to strengthen ceramics and increase density, smoothness, crack hardness, creep resistance, thermal fatigue resistance, and wear resistance. Its most common application is in integrated circuit baseboards. It has extremely high melting and boiling points of 29770°C and 20400°C, respectively, which increase the thermal inertia of the nanofluid [21]. Copper nanoparticles are a fascinating class of material with multifunctional properties that have prospective uses in catalysts, batteries, magnetic storage media, solar energy, and superconductors [22]. Because of their high surface area, these nanoparticles have significant benefits over traditional materials. Recently, researchers introduced a new kind of nanofluid, namely, "hybrid nanofluid" due to the demand for the high thermal conductivity and heat transfer rate by the growing technology of the world. Elasticity was predicted to be higher in thermal conductivity relative to standard fluid and nanofluid. The hybrid nanofluid concept is meant to describe a mix of superior properties at an acceptable expense with two or more specific forms of scattered nanoparticles in the base fluid. In this regard, many experimental and computational modified models have been purposed from these basic models [23–26]. Devi and Devi [27, 28] proposed a computational hybrid nanofluid model and concluded that it is the most appropriate model for the hybrid nanofluid by comparing the results with the practical investigational work of Suresh et al. [29]. Yan et al. [30] used the same properties of thermophysical and found double solutions over the exponential surface. This model has been used by many researchers to deal with the hybrid nanofluid such as [31–37].

In this study, the characteristics of flow and heat transfer of the hybrid nanofluid in the directions of streamwise and cross flow are investigated. To the best of the authors' knowledge, no such investigation on numerous solutions has previously been conducted. The current study has four main objectives: first, an analysis of the flow of the streamwise and cross-flow hybrid nanofluid model with thermal radiation impact, second, to adopt the Devi and Devi model for hybrid nanofluid, third, to obtain multiple branches, and fourth, to conduct a stability analysis.

2. Problem Formulation

Three-dimensional uniform steady transverse and streamwise flow of $Cu - Al_2O_3$/water hybrid nanofluid flow on the heated flat plate flowing with continual velocity $-\lambda U$ out and in of origin centered at $x = 0$ has been considered, where x is reference determined on a flat wall, U is the fixed velocity of the outward flow, and λ indicates the moving parameter. The constant temperature of the plate is T_w, whereas the uniform temperature of the free stream is T_∞ (refer Figure 1). It is, therefore, supposed that the cross-flow is infinite in the direction of spanwise and hence completely formed. The fields of temperature and velocity are thus independent of z coordinates, such that the boundary layer equation of energy with the term of thermal radiation may be written as follows [6, 34, 38]:

$$u_x + v_y = 0, \tag{1}$$

$$uu_x + vu_y = \frac{\mu_{\text{hnf}}}{\rho_{\text{hnf}}} u_{yy}, \tag{2}$$

$$uw_x + vw_y = \frac{\mu_{\text{hnf}}}{\rho_{\text{hnf}}} w_{yy}, \tag{3}$$

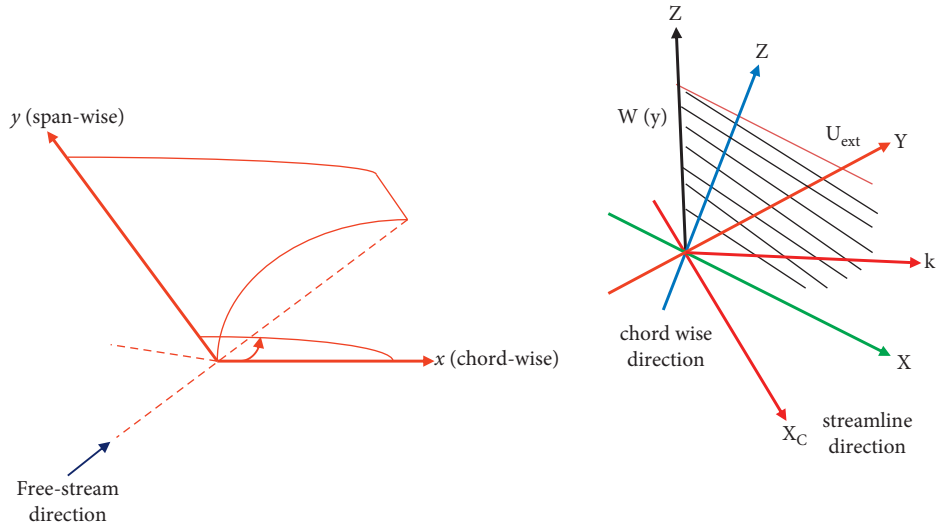

Figure 1: Coordinate system and model.

$$uT_x + vT_y = \frac{k_{\text{hnf}}}{(\rho c_p)_{\text{hnf}}} T_{yy} - \frac{1}{(\rho c_p)_{\text{hnf}}} \frac{\partial q_r}{\partial y}, \tag{4}$$

subject to the boundary conditions:

$$\begin{cases} v = 0, u = -\lambda U, w = 0; T = T_w \text{ at } y = 0, \\ u = U, w = W_0, T = T_\infty \text{ as } y \longrightarrow \infty, \end{cases} \tag{5}$$

where μ_{hnf}, $(c_p)_{\text{hnf}}$, ρ_{hnf}, and k_{hnf} are the dynamic viscosity, heat capacity, density, and thermal conductivity of hybrid nanofluid, respectively. Furthermore, subscription hnf indicates the thermophoresis properties of hybrid nanofluid. Moreover, y and z indicate the corresponding spanwise and normal coordinate in the direction of plane and transverse flow, corresponding velocity along x, y, and z axes is indicated by u, v, and w, the transverse velocity at origin is W_0, and the temperature of fluid is denoted by T. It should be noted that when $\lambda < 0$ ($\lambda > 0$), then plate passes out (into) of the origin. For this analysis, the unique type of properties of Yan et al. [30] is used to analyze the model of cross flow. Table 1 lists the thermophysical properties of the hybrid nanofluids that will be used in this study. Table 2 shows the thermophysical properties of water and nanoparticles.

Looking for similarity transformations to convert PDEs to ODEs, we have

$$\eta = y\left(\frac{U}{2\vartheta x}\right)^{1/2}, \psi = (2\vartheta x U)^{1/2} f(\eta), w = W_0 g(\eta), \quad \theta(\eta) = \frac{T - T_\infty}{T_w - T_\infty}. \tag{6}$$

Substituting equation (6) in equations (1)–(4), equation (1) is immediately satisfied, and equations (2)–(4) assume the following nondimensional form:

$$f''' + \xi_1 \xi_2 f f'' = 0, \tag{7}$$

$$g'' + \xi_1 \xi_2 f g' = 0, \tag{8}$$

$$\frac{1}{\text{Pr}}\left[\left(k_{\text{hnf}}/k_f\right)\xi_3 + \frac{4\text{Rd}}{3}\xi_3\right]\theta'' + f\theta' = 0, \tag{9}$$

subject to the boundary conditions:

$$\begin{cases} f(0) = 0, f'(0) = -\lambda, g(0) = 0, \theta(0) = 1, \\ f'(\eta) \longrightarrow 1, g(\eta) \longrightarrow 1, \theta \text{ as } (\eta) \longrightarrow 0 \text{ as } \eta \longrightarrow \infty, \end{cases} \tag{10}$$

where prime denotes the differentiation with respect to η; $\text{Pr} = \vartheta_f/\alpha_f$ denotes Prandtl number.

Table 1: Thermophysical properties of hybrid nanofluid.

Properties	Hybrid nanofluid
Dynamic viscosity	$\mu_{\mathrm{hnf}} = \mu_f/(1-\phi_{\mathrm{Cu}})^{2.5}(1-\phi_{\mathrm{Al_2O_3}})^{2.5}$
Density	$\rho_{\mathrm{hnf}} = (1-\phi_{\mathrm{Cu}})[(1-\phi_{\mathrm{Al_2O_3}})\rho_f + \phi_{\mathrm{Al_2O_3}}\rho_{\mathrm{Al_2O_3}}] + \phi_{\mathrm{Cu}}\rho_{\mathrm{Cu}}$
Thermal conductivity	$k_{\mathrm{hnf}} = (k_{\mathrm{Cu}} + 2k_{\mathrm{nf}} - 2\phi_{\mathrm{Cu}}(k_{\mathrm{nf}} - k_{\mathrm{Cu}})/k_{\mathrm{Cu}} + 2k_{\mathrm{nf}} + \phi_{\mathrm{Cu}}(k_{\mathrm{nf}} - k_{\mathrm{Cu}})) \times (k_{\mathrm{nf}})$, where $k_{\mathrm{nf}} = (k_{\mathrm{Al_2O_3}} + 2k_f - 2\phi_{\mathrm{Al_2O_3}}(k_f - k_{\mathrm{Al_2O_3}})/k_{\mathrm{Al_2O_3}} + 2k_f + \phi_{\mathrm{Al_2O_3}}(k_f - k_{\mathrm{Al_2O_3}})) \times (k_f)$
Heat capacity	$(\rho c_p)_{\mathrm{hnf}} = (1-\phi_{\mathrm{Cu}})[(1-\phi_{\mathrm{Al_2O_3}})(\rho c_p)_f + \phi_{\mathrm{Al_2O_3}}(\rho c_p)_{\mathrm{Al_2O_3}}] + \phi_{\mathrm{Cu}}(\rho c_p)_{\mathrm{Cu}}$
Electrical conductivity	$\sigma_{\mathrm{hnf}} = (\sigma_{\mathrm{Cu}} + 2\sigma_{\mathrm{nf}} - 2\phi_{\mathrm{Cu}}(\sigma_{\mathrm{nf}} - \sigma_{\mathrm{Cu}})/\sigma_{\mathrm{Cu}} + 2\sigma_{\mathrm{nf}} + \phi_{\mathrm{Cu}}(\sigma_{\mathrm{nf}} - \sigma_{\mathrm{Cu}})) \times (\sigma_{\mathrm{nf}})$, where $\sigma_{\mathrm{nf}} = (\sigma_{\mathrm{Al_2O_3}} + 2\sigma_f - 2\phi_{\mathrm{Al_2O_3}}(\sigma_f - \sigma_{\mathrm{Al_2O_3}})/\sigma_{\mathrm{Al_2O_3}} + 2\sigma_f + \phi_{\mathrm{Al_2O_3}}(\sigma_f - \sigma_{\mathrm{Al_2O_3}})) \times (\sigma_f)$

Table 2: Thermophysical properties of nanoparticles and water.

Fluids	Copper (Cu)	Alumina (Al_2O_3)	Water (H_2O)
ρ (kg/m^3)	8933	3970	997.1
c_p (J/kg K)	385	765	4179
k (W/m K)	400	40	0.613

$$\begin{cases} \xi_1 = \left\{(1-\phi_{\mathrm{Cu}})\left[1-\phi_{\mathrm{Al_2O_3}} + \phi_{\mathrm{Al_2O_3}}\left(\dfrac{\rho_{\mathrm{Al_2O_3}}}{\rho_f}\right)\right] + \phi_{\mathrm{Cu}}\left(\dfrac{\rho_{\mathrm{Cu}}}{\rho_f}\right)\right\}, \\ \xi_2 = (1-\phi_{\mathrm{Cu}})^{2.5}\left(1-\phi_{\mathrm{Al_2O_3}}\right)^{2.5}, \\ \xi_3 = \dfrac{1}{\left\{(1-\phi_{\mathrm{Cu}})\left[1-\phi_{\mathrm{Al_2O_3}} + \phi_{\mathrm{Al_2O_3}}\left(\rho c_p\right)_{\mathrm{Al_2O_3}}/\left(\rho c_p\right)_f\right] + \phi_{\mathrm{Cu}}\left(\rho c_p\right)_{\mathrm{Cu}}/\left(\rho c_p\right)_f\right\}}. \end{cases} \tag{11}$$

The physical quantities of interest are the coefficient of skin friction C_f and Nusselt number Nu_x which are described as

$$C_f = \frac{\mu_{\mathrm{hnf}}}{\rho_f U^2}\left(\frac{\partial u}{\partial y}\right)\Bigg| y=0, C_f = \frac{\mu_{\mathrm{hnf}}}{\rho_f W_0^2}\left(\frac{\partial w}{\partial y}\right)\Bigg| y=0, \mathrm{Nu}_x = -\frac{x k_{\mathrm{hnf}}}{k_f(T_w - T_\infty)}\left(\frac{\partial T}{\partial y}\right)\Bigg| y=0. \tag{12}$$

By putting equation (6) in equation (12), one obtains

$$\begin{aligned} \sqrt{2\mathrm{Re}}C_f &= \frac{1}{\left(1-\phi_{\mathrm{Al_2O_3}}\right)^{2.5}(1-\phi_{\mathrm{Cu}})^{2.5}} f''(0); \sqrt{\mathrm{Re}}C_f = \frac{1}{\left(1-\phi_{\mathrm{Al_2O_3}}\right)^{2.5}(1-\phi_{\mathrm{Cu}})^{2.5}} g'(0)\sqrt{\frac{\mathrm{Re}}{2}}\mathrm{Nu}_x \\ &= -\frac{k_{\mathrm{hnf}}}{k_f}\left[1+\frac{4\mathrm{Rd}}{3}\right]\theta'(0), \end{aligned} \tag{13}$$

where $\mathrm{Re} = Ux/\vartheta$ is the local Reynold number.

3. Stability Analysis

By taking the instructions of Khan et al. [39] to conduct a temporal study of reliability of branches, we ought to add a new nondimensional time-dependent similarity transformation by assuming $\tau = Ut/2x$ such that we have to obey new similarity transformation variables:

$$\begin{aligned} &\eta = y\left(\frac{U}{2\vartheta x}\right)^{1/2}, \tau = \frac{Ut}{2x}, \psi = (2\vartheta x U)^{1/2} f(\eta), \\ &w = W_0 g(\eta), \theta(\eta) = \frac{T - T_\infty}{T_w - T_\infty}. \end{aligned} \tag{14}$$

The unsteady model of the governing equations is written as

$$u_t + uu_x + vu_y = \frac{\mu_{\text{hnf}}}{\rho_{\text{hnf}}} u_{yy}, \tag{15}$$

$$w_t + uw_x + vw_y = \frac{\mu_{\text{hnf}}}{\rho_{\text{hnf}}} w_{yy}, \tag{16}$$

$$T_t + uT_x + vT_y = \frac{k_{\text{hnf}}}{\left(\rho c_p\right)_{\text{hnf}}} T_{yy} - \frac{1}{\left(\rho c_p\right)_{\text{hnf}}} \frac{\partial q_r}{\partial y}. \tag{17}$$

By replacing equation (14) in equations (15)–(17), we obtain

$$\frac{\partial^3 f}{\partial \eta^3} + \xi_1 \xi_2 \left\{ f \frac{\partial^2 f}{\partial \eta^2} - \frac{\partial^2 f}{\partial \tau \partial \eta} \right\} = 0, \tag{18}$$

$$\frac{\partial^2 g}{\partial \eta^2} + \xi_1 \xi_2 \left\{ f \frac{\partial g}{\partial \eta} - \frac{\partial g}{\partial \tau} \right\} = 0, \tag{19}$$

$$\frac{1}{\text{Pr}} \left[\left(k_{\text{hnf}} / k_f \right) \xi_3 + \frac{4\text{Rd}}{3} \xi_3 \right] \frac{\partial^2 \theta}{\partial \eta^2} + f \frac{\partial \theta}{\partial \eta} - \frac{\partial \theta}{\partial \tau} = 0, \tag{20}$$

subject to the boundary conditions:

$$\begin{cases} f(0,\tau) = 0, \dfrac{\partial f(0,\tau)}{\partial \eta} = -\lambda, g(0,\tau) = 0, \theta(0,\tau) = 1, \\ \dfrac{\partial f(\eta,\tau)}{\partial \eta} = 1, g(\eta,\tau) \longrightarrow 1, \theta(\eta,\tau) = 0 \text{ as } \eta \longrightarrow \infty. \end{cases} \tag{21}$$

To test the stability of steady flow branches, where $f(\eta) = f_0(\eta), \theta(\eta) = \theta_0(\eta)$, and $\varnothing(\eta) = \varnothing_0(\eta)$ satisfying BVP (7)–(9), it can be written as

$$\begin{cases} f(\eta,\tau) = f_0(\eta) + e^{-\gamma\tau} F(\eta,\tau), \\ w(\eta,\tau) = w_0(\eta) + e^{-\gamma\tau} S(\eta,\tau), \\ \theta(\eta,\tau) = \theta_0(\eta) + e^{-\gamma\tau} G(\eta,\tau), \end{cases} \tag{22}$$

where the corresponding small relatives of $f_0(\eta), w_0(\eta)$, and $\theta_0(\eta)$ are $F(\eta), S(\eta)$, and $G(\eta)$, and γ is an undefined eigenvalue quantity that needs to be calculated. Through replacing equation (22) in equations (18)–(20) with $\tau = 0$, we are presented with the following linearized problem of eigenvalue:

$$F_0''' + \xi_1 \xi_2 \{ f_0 F_0'' + F_0 f_0'' + \gamma F_0' \} = 0, \tag{23}$$

$$S_0'' + \xi_1 \xi_2 \{ f_0 S_0' + F_0 w_0' + \gamma S_0 \} = 0, \tag{24}$$

$$\frac{1}{\text{Pr}} \left[\left(k_{\text{hnf}} / k_f \right) \xi_3 + \frac{4\text{Rd}}{3} \xi_3 \right] G_0'' + f_0 G_0' + F_0 \theta_0' + \gamma G_0 = 0, \tag{25}$$

subject to boundary conditions:

$$\begin{cases} F_0(0) = 0, F_0'(0) = 0, S_0(0) = 0, G_0(0) = 0, \\ F_0'(\eta) = S_0(\eta) = G_0(\eta) \longrightarrow 0 \text{ as } \eta \longrightarrow \infty. \end{cases} \tag{26}$$

As per Khashi'ie et al. [33], one boundary condition must be modified to achieve the lowest γ_1. It should be remembered that there is no impact on the effects of this relaxation in boundary conditions [37]. For this specific problem, the boundary condition of $F_0'(\eta) \longrightarrow 0$ as $\eta \longrightarrow \infty$ is relaxed to $F_0''(0) = 1$.

4. Analysis and Discussion of Results

In this section, two branches have been obtained. Figure 2 portrays presence of the dual branches for a system of dimensionless ODEs (7)–(9) along with boundary conditions (10). These equations are solved by applying the III-stage-Lobatto-IIIa formula in bvp4c solver in MATLAB 2017 software. This technique has been commonly applied by various scholars and academics to get the solutions of the boundary layer problems. One must make an initial supposition at the initial mesh point and adjust the phase size in order to achieve the required consistency of the solutions. This method is explained extensively in the book of Shampine et al. [40].

The nondimensional profiles of streamwise velocity $f'(\eta)$, cross velocity $g(\eta)$, and temperature $\theta(\eta)$ are drawn in Figure 2 for numerous values of moving parameter ($\lambda > 0$) combinedly. It is detected that stream and cross velocities as well as temperature increase (decrease) in the upper (lower) branch when parameter of moving is augmented. However, thicknesses of momentum and thermal boundary layers are thicker in the lower solution as associated to the upper solution. Figure 3 shows the effect of λ on $f'(\eta)$ and $f(\eta)$. It can be observed easily that the profile of stream function is an increasing function of λ in the upper branch and vice versa.

Figures 4–6 demonstrate the behavior of $f'(\eta), g(\eta)$, and $\theta(\eta)$ for different values of ϕ_{Cu}, respectively. When volume fraction of Cu is augmented then velocity, cross-flow velocity and temperature of $\text{Cu} - \text{Al}_2\text{O}_3$/water hybrid nanofluid decrease in the upper as well as in lower branches as expected because lower thickness of the boundary helps to raise the heat transfer rate. Furthermore, the behavior of the thickness of the lower branch is the same as it is noticed in Figure 2.

Figure 7 is plotted for the effect of Pr on $\theta(\eta)$ when the values of the other all parameters are fixed. It is seen that the temperature profiles of $\text{Cu} - \text{Al}_2\text{O}_3$ /water hybrid nanofluid decline monotonically with the increment of Pr for the first solution. In the lower solution, thermal boundary layer thickness and temperature of $\text{Cu} - \text{Al}_2\text{O}_3$/water hybrid nanofluid rises at first and then tends to decline (refer to Figure 8). Figure 9 reveals that thickness of the thermal layer declines primarily and then enhances in the upper and lower solutions for the higher values of the thermal radiation parameter. It must be noted that when Rd = 0, lower branch does not converge at zero asymptotically. Therefore, it may

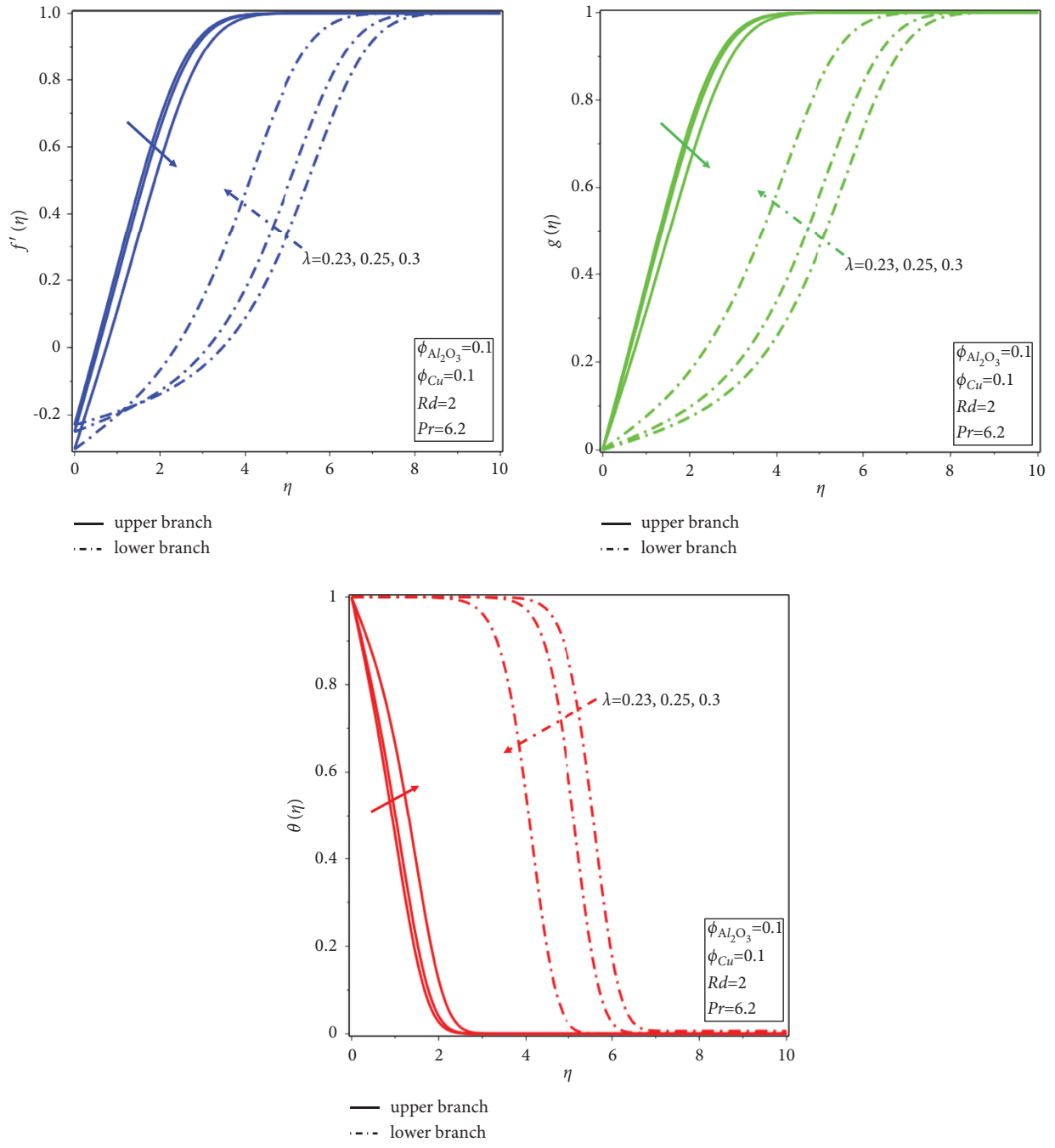

Figure 2: Effect of λ on $f'(\eta)$, $g(\eta)$, $\theta(\eta)$.

be stated that nonuniqueness solutions also depend on the thermal radiation parameter.

Figures 8–11 portray to check the behavior of $f''(0)$, $g'(0)$, and $-\theta'(0)$ against the volume fraction of the hybrid nanofluid (copper) for different values of λ. It has been noticed that two branches of solutions are obtained when the parameter $\lambda \geq 0.23$, while the behavior of the $f''(0)$ shows the existence of one branch when $\lambda < 0.23$. It must be distinguished that dual branches exist for $f''(0)$ and $g'(0)$ when $\lambda \geq 0.23$, but the profile of the temperature does not converge asymptotically at $\eta \longrightarrow \infty$; therefore, solutions of $f''(0)$ and $g'(0)$ could not be considered since we have solved the system of coupled ODEs. It is significant to remember that upper solution of dual branches is stable, whereas lower solution is unpredictable and unstable. These two branches are found in range $\lambda_c \geq \lambda \geq 0.23$, and $\lambda_c = 0.3541$ is a λ critical value where both branches exist, and it is the minimum value where solutions exist. The critical value of λ (i.e., $\lambda_c = 0.3541$) is the same as stated in article of Weidman et al. [6] which gives us the confidence to use our numerical method in this study. Furthermore, the

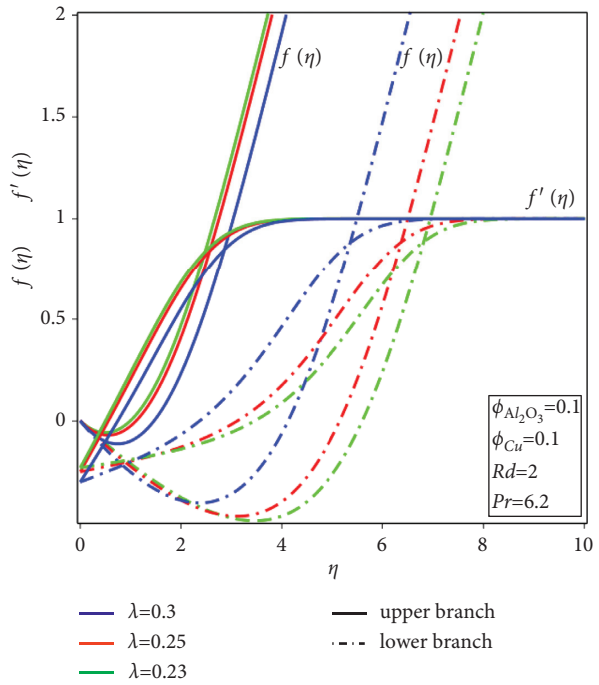

Figure 3: Effect of λ on velocity $f'(\eta)$ and reduced stream function $f(\eta)$.

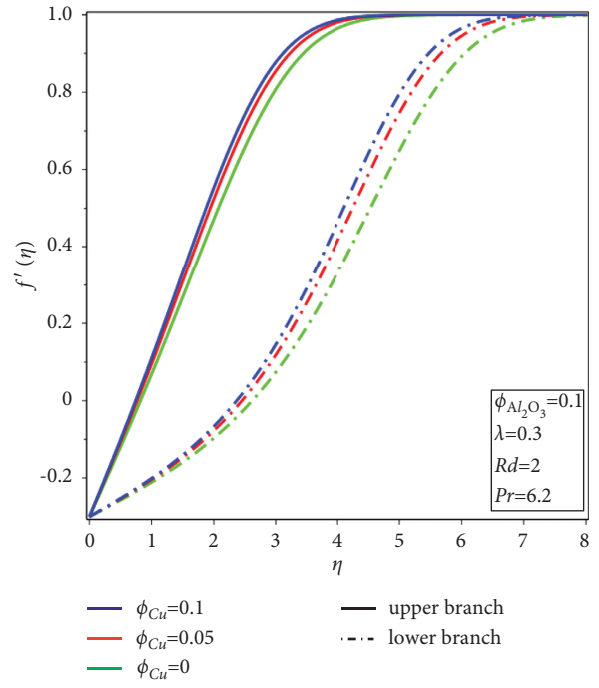

Figure 4: Effect of ϕ_{Cu} on $f'(\eta)$.

friction coefficient grows in upper branch for the higher values of λ (see Figure 8). Then, again, an opposite pattern is seen for $g'(0)$ and $-\theta'(0)$; however, the rate of heat transfer and skin friction boost as the volume fraction of the copper particles is enhanced during the examination of the $Cu - Al_2O_3$/water hybrid nanofluid (refer to Figures 10 and 11). In practice, increases in magnitude are caused by an increase in the heat capacity of the nanofluid, which can also be seen from the volume fraction relation shown in Tables 1 and 2.

At last, the linearized equations (23)–(25) along with boundary conditions (26) have been solved in order to perform the temporal stability of the upper and lower branches. Our goal of carrying out this analysis is to obtain

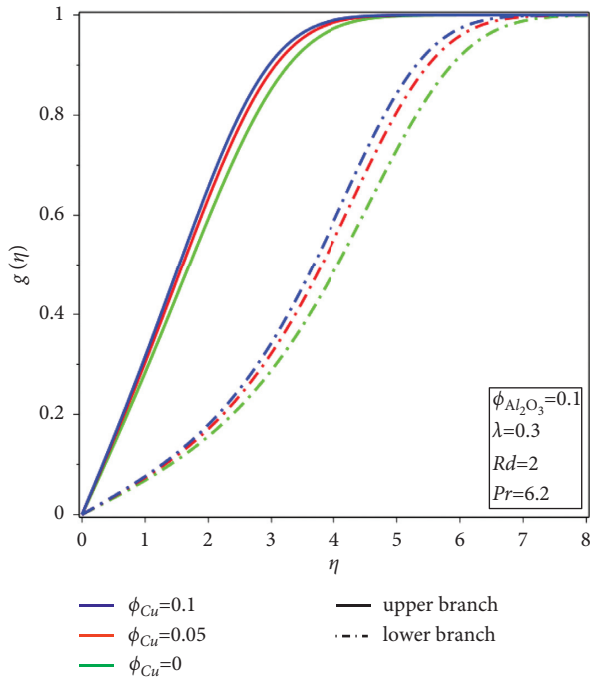

Figure 5: Effect of ϕ_{Cu} on cross-flow velocity $g(\eta)$.

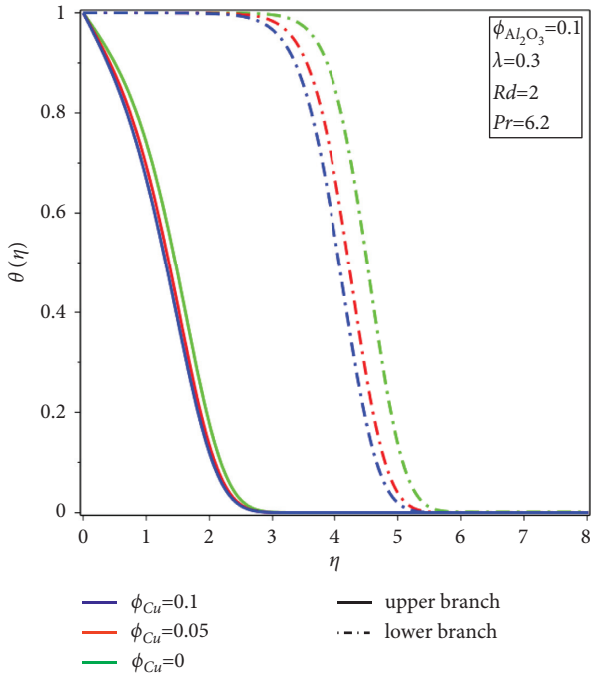

Figure 6: Effect of ϕ_{Cu} on temperature $\theta(\eta)$.

the minimum eigenvalue γ_1. The values of γ_1 are tabulated in Table 3. This is worth examining those values of γ_1 which are equal to zero when $\lambda = \lambda_c$. Henceforth, γ_1 changes sign from zero to positive for the upper branch (stable) and negative for the lower branch (unstable) which means that λ_c is a turning point.

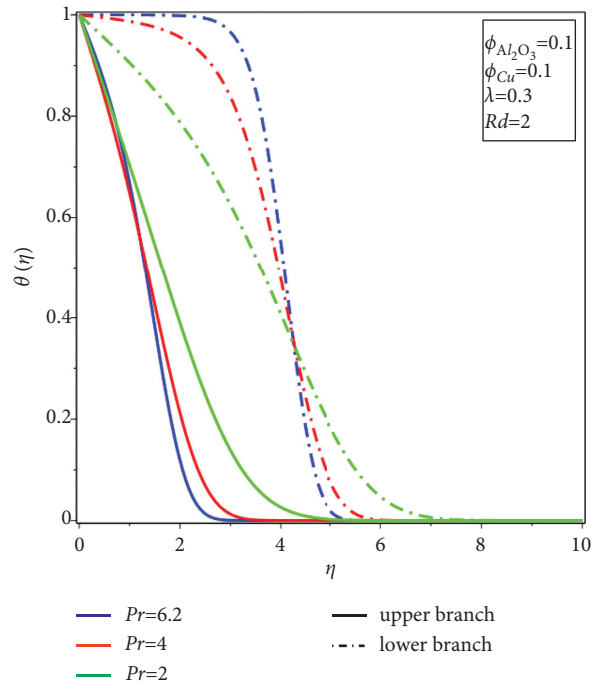

Figure 7: Effect of Pr on $\theta(\eta)$.

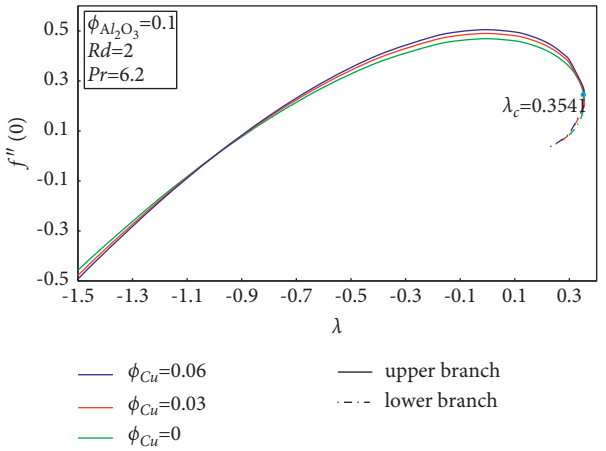

Figure 8: Effect of ϕ_{Cu} on skin friction coefficient $f''(0)$.

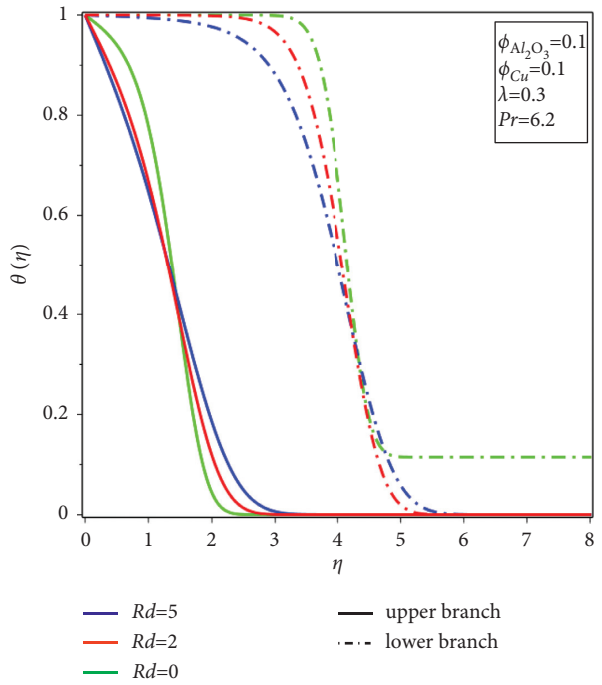

Figure 9: Effect of Rd on $\theta(\eta)$.

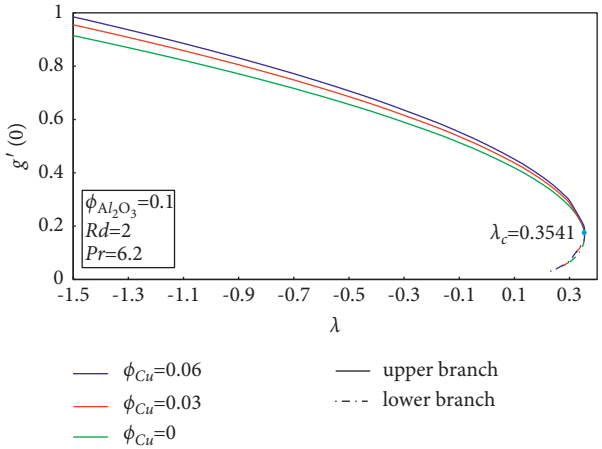

Figure 10: Effect of ϕ_{Cu} on skin friction coefficient $g'(0)$.

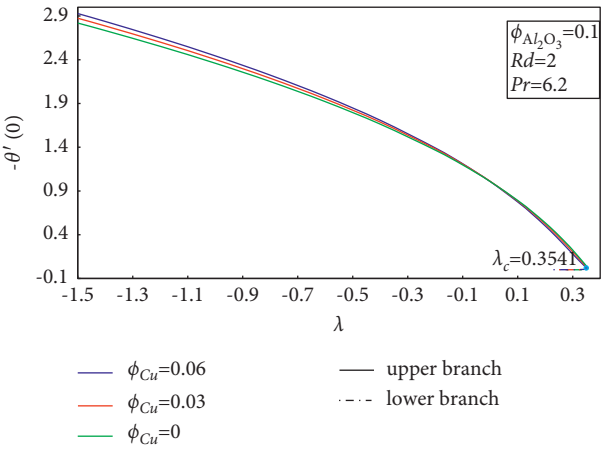

Figure 11: Effect of ϕ_{Cu} on heat transfer rate $-\theta'(0)$.

Table 3: γ_1 values for various values of moving parameter (λ), where $\phi_{Al_2O_3} = 0.1$, $\phi_{Cu} = 0.06$, Rd = 2, and Pr = 6.2.

λ	γ_1	
	Upper branch	Lower branch
−1	2.31031	—
−0.5	2.1106	—
0	1.81196	—
0.23	1.2736	−1.1496
0.25	1.0826	−1.0053
0.28	0.95325	−0.8205
0.3	0.52592	−0.4288
0.3541	0.03852	−0.0762

5. Conclusions

The heat transfer of the $Cu - Al_2O_3$/water type hybrid nanofluid of cross flow in the presence of radiation impacts was investigated. Similarity variables have been applied to change the governing equations into ODEs. The modified ODEs were then solved using the 3-stage Lobatto 3a method in bvp4c solver in MATLAB. The pointwise conclusion of this study is as follows:

(1) Dual branches depend on a certain range of λ

(2) There occur triple ranges of solution, no branch solution exists when $\lambda > \lambda_c$, two branches occur when $0.23 \leq \lambda \leq \lambda_c$, and a single branch exists when $\lambda > 0.23$

(3) The heat transfer improved due to the volume fraction of Cu in a hybrid nanofluid

(4) In the thermal radiation presence, the dual behavior is noted in the rate of heat transfer in both branches

(5) The results of stability analysis suggest that upper branch is feasible and stable; the lower branch is unrealizable and unstable

Nomenclature

Al_2O_3: Aluminum oxide
T_∞: Ambient temperature
k^*: Coefficient of mean absorption
Cu: Copper
ρ_{hnf}: Density of hybrid nanofluid
θ: Dimensionless temperature
f', g: Dimensionless velocity
μ_{hnf}: Dynamic viscosity of hybrid nanofluid
T: Fluid temperature
W_0: Transverse velocity
Nu_x: Local Nusselt number
Re: Local Reynolds number
ODEs: Ordinary differential equations
PDEs: Partial differential equations
Pr: Prandtl number
q_r: Radiation flux
C_{fx}, C_{fz}: Skin friction coefficient
γ: Unknown eigenvalue
γ_1: Smallest eigenvalue
$(\rho c_p)_{hnf}$: Heat capacity of hybrid nanofluid
τ: Stability similarity variable
ψ: Stream function
λ: Moving parameter
U: Constant outward flow velocity
k_{hnf}: Thermal conductivity of hybrid nanofluid
Rd: Thermal radiation
t: Time
σ_1: Stefan–Boltzmann constant
η: Similarity variable
T_w: Variable temperature at the sheet
x, y, z: Cartesian coordinates
u, v, w: Velocity components
ϕ: Volume fraction
H_2O: Water.

Data Availability

The data that support the findings of this study are available from the corresponding author upon reasonable request.

Conflicts of Interest

The authors declare that they have no conflicts of interest.

References

[1] L. Sowerby, "Secondary flow in a boundary layer," *Report Aeronautical Research Council Lond*, p. 16832, 1954.

[2] J. B. Klemp and A. Acrivos, "A method for integrating the boundary-layer equations through a region of reverse flow," *Journal of Fluid Mechanics*, vol. 53, no. 1, pp. 177–191, 1972.

[3] J. B. Klemp and A. Acrivos, "A moving-wall boundary layer with reverse flow," *Journal of Fluid Mechanics*, vol. 76, no. 2, pp. 363–381, 1976.

[4] M. Y. Hussaini, W. D. Lakin, and A. Nachman, "On similarity solutions of a boundary layer problem with an upstream moving wall," *SIAM Journal on Applied Mathematics*, vol. 47, no. 4, pp. 699–709, 1987.

[5] Z. Altaç, Z. Sert, N. Mahir, and Ç. Timuralp, "Mixed convection heat transfer from a triangular cylinder subjected to upward cross flow," *International Journal of Thermal Sciences*, vol. 137, pp. 75–85, 2019.

[6] P. D. Weidman, "New solutions for laminar boundary layers with cross flow," *Zeitschrift für Angewandte Mathematik und Physik*, vol. 48, no. 2, pp. 341–356, 1997.

[7] T. Fang, "Similarity solutions for a moving-flat plate thermal boundary layer," *Acta Mechanica*, vol. 163, no. 3-4, pp. 161–172, 2003.

[8] T. Fang, "Further study on a moving-wall boundary-layer problem with mass transfer," *Acta Mechanica*, vol. 163, no. 3-4, pp. 183–188, 2003.

[9] T. Fang and C.-f. F. Lee, "Three-dimensional wall-bounded laminar boundary layer with span-wise cross free stream and moving boundary," *Acta Mechanica*, vol. 204, no. 3-4, pp. 235–248, 2009.

[10] F. Tie-Gang, Z. Ji, and Y. Shan-Shan, "Viscous flow over an unsteady shrinking sheet with mass transfer," *Chinese Physics Letters*, vol. 26, no. 1, Article ID 014703, 2009.

[11] M. Sheikholeslami, M. Jafaryar, A. Shafee, and H. Babazadeh, "Acceleration of discharge process of clean energy storage unit with insertion of porous foam considering nanoparticle enhanced paraffin," *Journal of Cleaner Production*, vol. 261, Article ID 121206, 2020.

[12] M. Sheikholeslami, A. N. Keshteli, and H. Babazadeh, "Nanoparticles favorable effects on performance of thermal storage units," *Journal of Molecular Liquids*, vol. 300, Article ID 112329, 2020.

[13] S. U. Choi and J. A. Eastman, *Enhancing Thermal Conductivity of Fluids with Nanoparticles*, Argonne National Lab., Detroit, IL, USA, 1995.

[14] I. L. Animasaun, B. Mahanthesh, A. O. Jagun et al., "Significance of Lorentz force and thermoelectric on the flow of 29 nm CuO–water nanofluid on an upper horizontal surface of a paraboloid of revolution," *Journal of Heat Transfer*, vol. 141, no. 2, 2019.

[15] M. K. A. Mohamed, A. Hussanan, H. T. Alkasasbeh, B. Widodo, and M. Z. Salleh, "Boundary layer flow on permeable flat surface in Ag-Al2O3/water hybrid nanofluid with viscous dissipation," *Data Analytics and Applied Mathematics (DAAM)*, vol. 2, no. 1, pp. 11–19, 2021.

[16] G. Rasool and T. Zhang, "Darcy-Forchheimer nanofluidic flow manifested with Cattaneo-Christov theory of heat and mass flux over non-linearly stretching surface," *PLoS One*, vol. 14, no. 8, Article ID e0221302, 2019.

[17] G. Rasool and A. Wakif, "Numerical spectral examination of EMHD mixed convective flow of second-grade nanofluid towards a vertical Riga plate using an advanced version of the revised Buongiorno's nanofluid model," *Journal of Thermal Analysis and Calorimetry*, vol. 143, pp. 1–15, 2020.

[18] W. A. Khan, A. M. Rashad, S. M. M. EL-Kabeir, and A. M. A. EL-Hakiem, "Framing the MHD micropolar-nanofluid flow in natural convection heat transfer over a radiative truncated cone," *Processes*, vol. 8, no. 4, p. 379, 2020.

[19] A. Shafiq, I. Zari, G. Rasool, I. Tlili, and T. S. Khan, "On the MHD Casson axisymmetric Marangoni forced convective flow of nanofluids," *Mathematics*, vol. 7, no. 11, p. 1087, 2019.

[20] S. R. Smith, R. Rafati, A. Sharifi Haddad, A. Cooper, and H. Hamidi, "Application of aluminium oxide nanoparticles to enhance rheological and filtration properties of water based muds at HPHT conditions," *Colloids and Surfaces A: Physicochemical and Engineering Aspects*, vol. 537, pp. 361–371, 2018.

[21] Y.-Q. Song, B. D. Obideyi, N. A. Shah, I. L. Animasaun, Y. M. Mahrous, and J. D. Chung, "Significance of haphazard motion and thermal migration of alumina and copper nanoparticles across the dynamics of water and ethylene glycol on a convectively heated surface," *Case Studies in Thermal Engineering*, vol. 26, Article ID 101050, 2021.

[22] J. Garg, B. Poudel, M. Chiesa et al., "Enhanced thermal conductivity and viscosity of copper nanoparticles in ethylene glycol nanofluid," *Journal of Applied Physics*, vol. 103, no. 7, Article ID 074301, 2008.

[23] D. A. G. Bruggeman, "Berechnung verschiedener physikalischer Konstanten von heterogenen Substanzen. I. Dielektrizitätskonstanten und Leitfähigkeiten der Mischkörper aus isotropen Substanzen," *Annalen der Physik*, vol. 416, no. 7, pp. 636–664, 1935.

[24] J. C. Maxwell, *Electricity and Magnetism*, Vol. 2, Dover, , New York, NY, USA, 1954.

[25] A. Einstein, "On the theory of the Brownian movement," *Annals of Physics*, vol. 19, no. 4, pp. 371–381, 1906.

[26] H. C. Brinkman, "The viscosity of concentrated suspensions and solutions," *The Journal of Chemical Physics*, vol. 20, no. 4, p. 571, 1952.

[27] S. P. A. Devi and S. S. U. Devi, "Numerical investigation of hydromagnetic hybrid Cu–Al_2O_3/water nanofluid flow over a permeable stretching sheet with suction," *International Journal of Nonlinear Sciences and Numerical Stimulation*, vol. 17, no. 5, pp. 249–257, 2016.

[28] S. U. Devi and S. A. Devi, "Heat transfer enhancement of cu–$ al_ {2} o_ {3} $/water hybrid nanofluid flow over a stretching sheet," *Journal of the Nigerian Mathematical Society*, vol. 36, no. 2, pp. 419–433, 2017.

[29] S. Suresh, K. P. Venkitaraj, P. Selvakumar, and M. Chandrasekar, "Synthesis of Al_2O_3–Cu/water hybrid nanofluids using two step method and its thermo physical properties," *Colloids and Surfaces A: Physicochemical and Engineering Aspects*, vol. 388, no. 1-3, pp. 41–48, 2011.

[30] L. Yan, S. Dero, I. Khan et al., "Dual solutions and stability analysis of magnetized hybrid nanofluid with joule heating and multiple slip conditions," *Processes*, vol. 8, no. 3, p. 332, 2020.

[31] I. Waini, A. Ishak, and I. Pop, "Hybrid nanofluid flow towards a stagnation point on a stretching/shrinking cylinder," *Scientific Reports*, vol. 10, no. 1, pp. 9296–9312, 2020.

[32] N. S. Khashi'ie, N. M. Arifin, I. Pop, and N. S. Wahid, "Flow and heat transfer of hybrid nanofluid over a permeable shrinking cylinder with Joule heating: a comparative analysis," *Alexandria Engineering Journal*, vol. 59, 2020.

[33] N. S. Khashi'ie, N. M. Arifin, E. H. Hafidzuddin, and N. Wahi, "Thermally stratified flow of Cu-Al2O3/water hybrid nanofluid past a permeable stretching/shrinking circular cylinder," *Journal of Advanced Research in Fluid Mechanics and Thermal Science*, vol. 63, pp. 154–163, 2019.

[34] R. K. Tiwari and M. K. Das, "Heat transfer augmentation in a two-sided lid-driven differentially heated square cavity utilizing nanofluids," *International Journal of Heat and Mass Transfer*, vol. 50, no. 9-10, pp. 2002–2018, 2007.

[35] L. Ali Lund, D. L. C. Ching, Z. Omar, I. Khan, and K. S. Nisar, "Triple local similarity solutions of Darcy-Forchheimer Magnetohydrodynamic (MHD) flow of micropolar nanofluid over an exponential shrinking surface: stability analysis," *Coatings*, vol. 9, no. 8, p. 527, 2019.

[36] N. S. Khashi'ie, N. M. Arifin, M. M. Rashidi, E. H. Hafidzuddin, and N. Wahi, "Magnetohydrodynamics (MHD) stagnation point flow past a shrinking/stretching surface with double stratification effect in a porous medium," *Journal of Thermal Analysis and Calorimetry*, vol. 139, pp. 1–14, 2019.

[37] I. Waini, A. Ishak, and I. Pop, "Transpiration effects on hybrid nanofluid flow and heat transfer over a stretching/shrinking sheet with uniform shear flow," *Alexandria Engineering Journal*, vol. 59, no. 1, pp. 91–99, 2020.

[38] F. A. Soomro, Z. H. Khan, and Q. M. Al-Mdallal, "Numerical study of streamwise and cross flow in the presence of heat and mass transfer," *The European Physical Journal Plus*, vol. 132, no. 5, pp. 1–9, 2017.

[39] U. Khan, I. Waini, A. Ishak, and I. Pop, "Unsteady hybrid nanofluid flow over a radially permeable shrinking/stretching surface," *Journal of Molecular Liquids*, vol. 331, Article ID 115752, 2021.

[40] L. F. Shampine, I. Gladwell, L. Shampine, and S. Thompson, *Solving ODEs with Matlab*, Cambridge University Press, Cambridge, MA, USA, 2003.